Topological Magnon Bands in a Kagome Lattice Ferromagnet

R. Chisnell, J. S. Helton, D. E. Freedman, D. K. Singh, R. I. Bewley, D. G. Nocera, and Y. S. Lee

Phys. Rev. Lett. **115**, 147201 — Published 28 September 2015

DOI: 10.1103/PhysRevLett.115.147201

Topological magnon bands in a kagome lattice ferromagnet

R. Chisnell,[1,2,*] J. S. Helton,[2] D. E. Freedman,[3,4] D. K. Singh,[5] R. I. Bewley,[6] D. G. Nocera,[3,7] and Y. S. Lee[1,8,†]

[1]*Department of Physics, Massachusetts Institute of Technology, Cambridge, MA 02139*

[2]*NIST Center for Neutron Research, Gaithersburg, MD 20899*

[3]*Department of Chemistry, Massachusetts Institute of Technology, Cambridge, MA 02139*

[4]*Department of Chemistry, Northwestern University, Evanston, IL 60208*

[5]*Department of Physics and Astronomy, University of Missouri, Columbia, MO 65211*

[6]*ISIS Facility, Rutherford Appleton Laboratory, Chilton, Didcot, OX11 0QX, Oxfordshire, UK*

[7]*Department of Chemistry and Chemical Biology, Harvard University, Cambridge, MA 02138*

[8]*Department of Applied Physics and Department of Photon Science, Stanford University and SLAC National Accelerator Laboratory, Stanford, CA 94305*

(Dated: September 8, 2015)

Abstract

There is great interest in finding materials possessing quasiparticles with topological properties. Such materials may have novel excitations that exist on their boundaries which are protected against disorder. We report experimental evidence that magnons in an insulating kagome ferromagnet can have a topological band structure. Our neutron scattering measurements further reveal that one of the bands is flat due to the unique geometry of the kagome lattice. Spin wave calculations show that the measured band structure follows from a simple Heisenberg Hamiltonian with a Dzyaloshinkii-Moriya interaction. This serves as the first realization of an effectively two-dimensional topological magnon insulator – a new class of magnetic material that should display both a magnon Hall effect and protected chiral edge modes.

When quantum particles are confined to move in reduced dimensions, such as in planes, unexpectedly rich physics can emerge as a result of the geometry and interactions. The quantum Hall effect is a famous example, which results from placing a two-dimensional (2D) gas of electrons or quasiparticles in a large magnetic field [1]. Pioneering theoretical work by Haldane showed that some systems may inherently possess topological bands that allow them to exhibit quantum Hall physics without applied magnetic fields [2]. The discovery of materials in which strong spin-orbit coupling leads to topological bands, such as topological insulators, has led to a flurry of activity in condensed matter physics research [3, 4]. Recently, theoretical studies have focused on 2D topological band structures that include flat bands due to the possibility of achieving fractional quantum hall physics in the absence of magnetic fields [5]. Flat bands (bands that are dispersionless in energy) hold unique interest because the interaction energy between particles may dominate the kinetic energy, leading to novel correlated electron states. A number of theoretical models for the fractional quantum Hall effect have been proposed based on flat topological bands [6–8]; however, these invariably require tuning of parameters, which is difficult to control in real materials.

Topological band structures are not unique to systems with electron-like quasiparticles. It has been demonstrated that topological photon modes can be realized in experimental systems [9–11]. Possible realizations of topological bosonic systems that include flat bands have been proposed using dipolar molecules trapped in an optical lattice [12], and using photonic lattices [13] based on the interaction between photons and arrays of superconducting circuits [14], although experimental confirmation has yet to be demonstrated. In this report, we show that topological bands exist for another class of quasiparticles: magnons in an insulating ferromagnet. Our material serves as the first realization of an effectively 2D topological magnon insulator [15], an electrically insulating state in which the spin degrees of freedom display properties analagous to those of the electric degrees of freedom in electronic topological insulators. Here, the magnons display a bulk band gap with gapless, nondissipative edge modes within the bulk gap. Thus magnons in our material should display novel behavior, such as a magnon Hall effect and chiral motion on the edge. Although we note that, as magnons are bosons, we do not expect a quantized Hall effect, this novel behavior has possible applications to the field of spintronics [16] where spin currents may be exploited for energy efficient technologies.

The kagome lattice ferromagnet provides an ideal system in which to investigate the

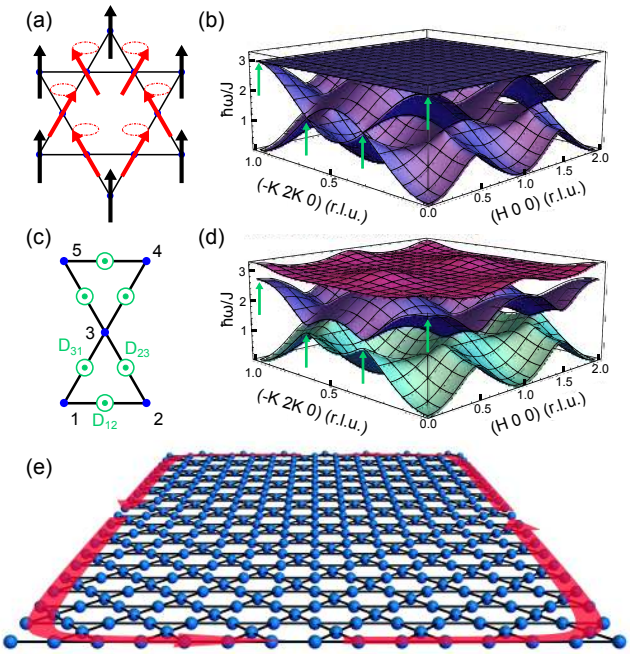

FIG. 1. (Color Online) Spin wave excitations in the kagome lattice ferromagnet. (a) A localized spin wave excitation supported by the kagome lattice. Due to the kagome geometry, excited (red) spins are decoupled from the rest of the lattice because a rotation of the neighboring ground-state (black) spins does not lower the overall energy of the spin configuration. Dashed lines indicate the excited spin precession path. (b) The spin wave dispersion of the kagome lattice ferromagnet, which consists of two dispersive modes and a perfectly flat mode, corresponding to the localized excitation shown in (a). Arrows show the locations of touch points between neighboring bands along $[-K\ 2K\ 0]$. (c) Out-of-plane component of the Dzyaloshinskii-Moriya (DM) vectors (D_z) on the kagome lattice, which have the same direction and magnitude for every bond because of the lattice symmetries. (d) Dispersion of the Heisenberg ferromagnet with DM interaction on the kagome lattice with $D_z/J = 0.15$. Arrows are at the same locations as in (b) and show the gaps that open between bands due to the DM interaction. (e) Topologically protected chiral magnon edge modes. Magnons propagate around the edge of the lattice in a single direction.

behavior of flat, topological magnon bands. The geometry of the kagome lattice leads to the existence of localized excitations, and therefore to dispersionless excitation bands [17]. It is well known that the kagome lattice antiferromagnet has a flat spin wave mode due to geometrical spin frustration [18]. For the kagome ferromagnet, a flat mode also exists; however, it occurs for the highest energy band. A localized spin wave in the kagome

ferromagnet is depicted in Fig. 1(a), showing an excitation around a hexagon of the kagome lattice. This excitation is decoupled from the rest of the lattice by frustrated hopping amplitudes to neighboring vertices. Figure 1(b) shows the dispersion of the spin wave excitation spectrum for the nearest-neighbor Heisenberg model on the kagome lattice, where one notes the perfectly flat band on top, which corresponds to the localized excitation. One also sees that the middle band is dispersive and meets the flat band at quadratic touching points. Interestingly, these touching points are protected by real space topology [17], where additional interaction terms may open a gap only if they remove the perfect flatness of the top band.

Using inelastic neutron scattering, we directly measure the spin wave dispersion relations in a kagome ferromagnet. The material that we study is Cu(1,3-benzenedicarboxylate(bdc)), a metal-organic framework compound featuring $S = 1/2$ Cu^{2+} ions with an ideal kagome lattice geometry [19]. The lack of inversion symmetry between magnetic Cu ions allows for an additional Dzyaloshinskii-Moriya (DM) interaction. Our results show that this additional perturbation is responsible for opening up gaps between the three magnon bands when the magnetic moments are aligned out of the kagome plane [20], as shown in Figure 1(d). Most interestingly, this type of interaction should yield topologically nontrivial bulk bands with resultant boundary modes that allow for chiral magnon transport on the edge [15], as schematically depicted in Fig. 1(e). Additionally, the DM interaction results in a Hall effect for the bulk magnons, as has been observed in ferromagnetic materials with a pyrochlore lattice, a 3D lattice containing kagome planes along the [111] direction [21, 22].

Neutron experiments were performed on a $\vec{c}$ axis-aligned sample of Cu(1,3-bdc), which was deuterated [23]. Measurements were taken with a magnetic field applied perpendicular to the kagome plane on the time-of-flight spectrometer LET at the Rutherford Lab [24], and with a magnetic field applied parallel to the kagome plane on the triple-axis spectrometer SPINS at the NIST Center for Neutron Research. Figure 2(a) shows scans through the magnetic Bragg peak (0 0 1) at $T = 70$ mK. Application of a small magnetic field shifts the intensity to (0 0 even)-type reflections, as shown in Fig. 2(b). This indicates that in Cu(1,3-bdc), below $T = 1.77$ K, the magnetic moments order ferromagnetically within each kagome plane, with a weak antiferromagnetic coupling between adjacent planes, as shown schematically in Fig. 2(c). A small magnetic field ($\mu_0 H \approx 0.05$ T) can fully polarize the moments in the direction of the applied field, as shown in Fig. 2(d), consistent with earlier

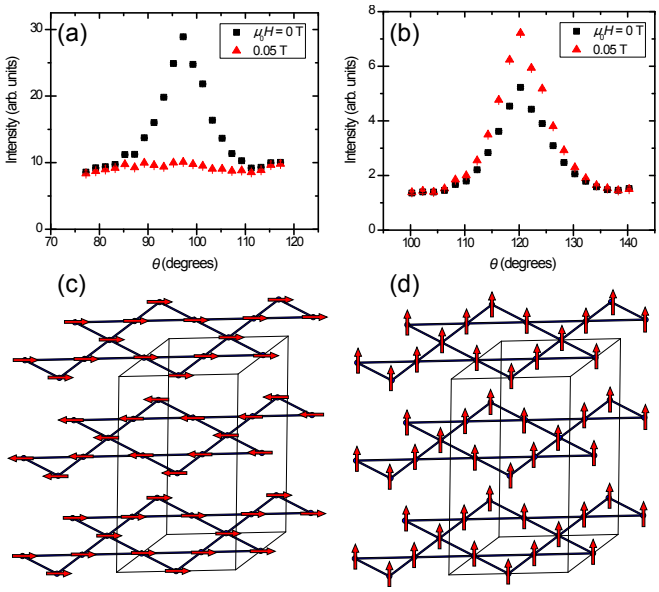

FIG. 2. (Color Online) Ground state spin configuration of Cu(1,3-bdc). (a)/(b) Elastic neutron scattering scans through the magnetic Bragg peaks measured at $T = 70$ mK at the (a) (0 0 1) and (b) (0 0 4) Bragg positions. Application of a magnetic field parallel to the kagome plane quickly suppresses the Bragg peak at (0 0 1) and increases intensity of the Bragg peak at (0 0 4). (c)/(d) Ground state spin configuration of Cu(1,3-bdc), where spin-1/2 Cu^{2+} ions form a kagome lattice. (c) Zero magnetic field configuration. Spins within each plane are ordered ferromagnetically, and neighboring planes ordered antiferromagnetically. Spins point parallel to the kagome plane. (d) A small magnetic field can polarize and reorient all spins in the direction of the applied field. Here the field is applied perpendicular to the kagome plane.

magnetization measurements [19]. For this system, the structurally perfect kagome lattice, the absence of other species of metal ion, and the weak interlayer coupling make it ideal for examining fundamental physics with a simple spin Hamiltonian.

Figure 3 shows inelastic neutron scattering intensities as a function of momentum and energy transfer at various applied magnetic field strengths, with the field applied perpendicular to the kagome plane. At zero applied field, we observe a dispersive excitation extending from zero energy and momentum transfer up to $|\vec{Q}| \approx 0.8$ Å^{-1}, $\hbar\omega \approx 1.8$ meV where it connects with a flat excitation. For $H = 0$, the width of the flat band is broader than the instrumental energy resolution. In the applied magnetic fields, the spectrum sharpens and is shifted to higher energies by an amount given by the Zeeman energy $g\mu_B H$. At the same

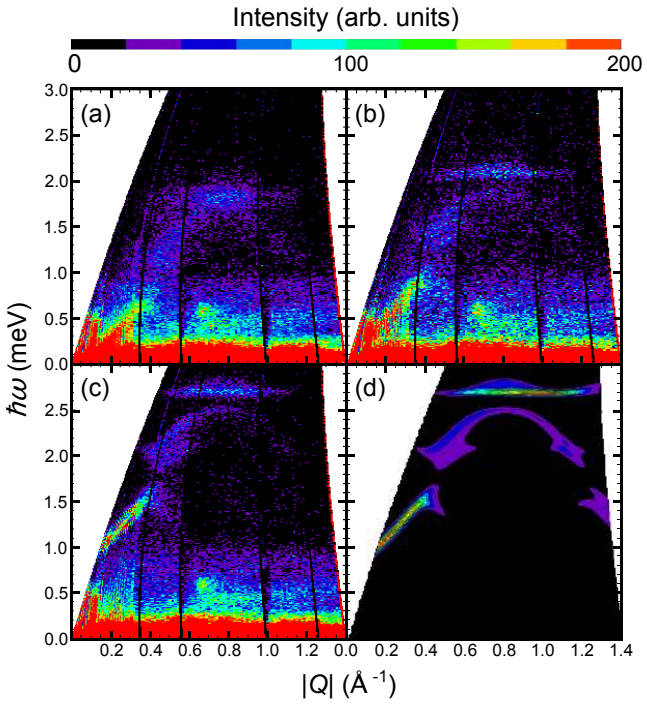

FIG. 3. (Color Online) Magnon dispersion in Cu(1,3-bdc). (a) – (c) Inelastic neutron scattering spectrum measured on LET with incident neutron energy 6.01 meV at $T = 1$ K and (a) zero field and applied fields (b) 2 T and (c) 7 T with the field applied perpendicular to the kagome plane. Black stripes are due to missing detectors. (d) Calculated inelastic structure factor for the Heisenberg ferromagnet with DM interaction convolved with the instrumental resolution function with parameters $J = 0.6$ meV, $g_z = 2.2$, $D_z = 0.09$ meV, and $\mu_0 H = 7$ T, and displayed over the measureable range for the LET spectrometer. $|Q|$ is the magnitude of the momentum transfer vector parallel to the kagome plane.

time, gaps open in the excitation spectrum forming three distinct bands. The highest energy band remains nearly flat, broadening slightly as $|\vec{Q}|$ approaches 0.8 Å^{-1}. No significant magnetic scattering was observed at energies above this flat excitation band.

The inelastic scattering spectrum of Cu(1,3-bdc) displays a strong dependence on the direction of the applied magnetic field. Figure 4(a) and 4(b) compares scattering intensities with the field applied perpendicular to and parallel to the kagome plane. In contrast to the measurement taken with the field applied perpendicular to the kagome plane, when the field is applied parallel to the kagome plane, no gap opens between the flat mode and the lower energy dispersive mode as the field is applied.

We model this system as a nearest-neighbor Heisenberg ferromagnet with DM interaction. The Hamiltonian can be written as:

$$\mathcal{H} = \sum_{\langle i,j \rangle} \left[-J\vec{S}_i \cdot \vec{S}_j + \vec{D}_{ij} \cdot \left(\vec{S}_i \times \vec{S}_j \right) \right] - g\mu_B \vec{H} \cdot \sum_i \vec{S}_i \tag{1}$$

where $\vec{S}_i$ is the Cu^{2+} spin moment at site i, $\vec{D}_{ij}$ is the DM vector between sites i and j, and $\langle i,j \rangle$ indicates summation over pairs of nearest-neighbor Cu atoms. The final term is the Zeeman energy from coupling to the applied magnetic field $\vec{H}$. Figure 1(c) shows the out-of-plane component of the DM vector, D_z, on the kagome lattice allowed by the symmetries of the Cu(1,3-bdc) crystal lattice according to Moriya's rules [25]. Since the DM interaction is antisymmetric under the exchange of two spins, is defined relative to the order in which we consider the spins. We define $\vec{D}_{ij}$ such that, for the triangle with vertices labeled 1, 2, and 3 in Fig. 1(c), the contribution to the Hamiltonian is of the form $\vec{D}_{12} \cdot \left(\vec{S}_1 \times \vec{S}_2 \right) + \vec{D}_{23} \cdot \left(\vec{S}_2 \times \vec{S}_3 \right) + \vec{D}_{31} \cdot \left(\vec{S}_3 \times \vec{S}_1 \right)$. In this manner we consider the spins in a counter-clockwise order around a triangle.

To calculate the spin wave dispersion, we use the Holstein-Primakoff transformation [26] to represent this Hamiltonian as a bosonic hopping model. Components of the DM vector perpendicular to the spin polarization direction (set by the applied magnetic field direction $\hat{z} = \vec{H}/H$) do not affect the Hamiltonian to quadratic order in deviation of $\vec{S}$ [21]. When the magnetic field is applied perpendicular to the kagome plane, we include only the out-of-plane component of the DM vector, $\vec{D}_{ij} \cdot \hat{z} = \pm D_z$.

The calculated dispersion is shown in Fig. 1(d). This model is equivalent the model considered by Zhang *et al.* [15]. The top and bottom bands are topologically nontrivial for $D_z \neq 0$; that is, the Berry curvature of the magnon bands results in Chern numbers of -1, 0, and +1 for the lowest, middle, and highest energy bands, respectively. To compare with our neutron scattering data, we calculated the dynamic structure factor for the spin waves, $\mathbf{S}_{\mathrm{SW}}(\vec{\mathbf{Q}}, \omega)$, which is proportional to the inelastic scattering intensity. This function was averaged over $\hat{Q}$ directions in the kagome plane and then convolved with the instrumental resolution function.

Figure 3(d) shows the calculated $\mathbf{S}_{\mathrm{SW}}(\vec{\mathbf{Q}}, \omega)$ for $\mu_0 H = 7$ T with $J = 0.6$ meV and $D_z = 0.09$ meV, which has good qualitative agreement with the observed intensity at 7 T (Fig. 3(c)). To compare our model quantitatively with the data, we employ the following analysis which allows us to fit the data while removing the effects of nonmagnetic background.

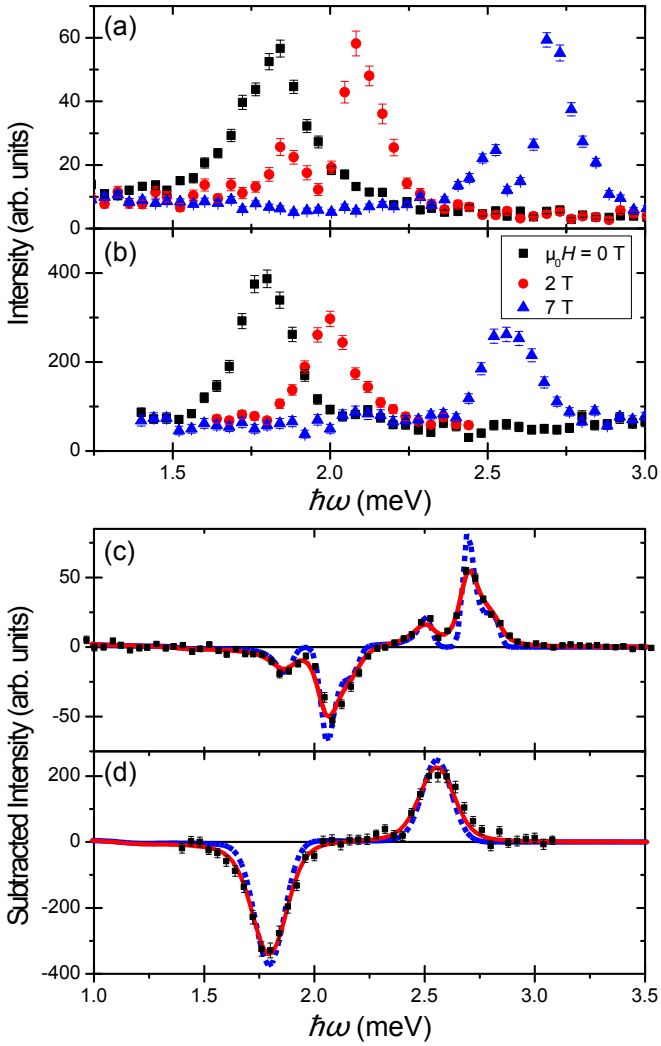

FIG. 4. (Color Online) Dependence of the magnon dispersion on applied field direction. (a) Magnetic field applied perpendicular to the kagome plane. Data were taken on LET and integrated over the momentum transfer range 0.72 $\text{Å}^{-1} \leq |\vec{Q}| \leq 0.88$ Å^{-1}. (b) Magnetic field applied parallel to the kagome plane. Data were taken on SPINS at $|\vec{Q}| = 0.8\text{Å}^{-1}$ with a $|\vec{Q}|$-resolution of ~ 0.15 Å^{-1}. (c)/(d) Quantitative comparison to the deduced spin Hamiltonian. The data points in (c) correspond to the difference in intensities at $\mu_0 H = 7$ T and $\mu_0 H = 2$ T with the field perpendicular to the plane, and the data points in (d) correspond to the difference in intensities at $\mu_0 H = 7$ T and $\mu_0 H = 0$ T with the field parallel to the plane. The lines denote the calculated structure factor for the Heisenberg ferromagnet with DM interaction integrated over the same values of $|\vec{Q}|$ as the data and convolved with the instrumental resolution function, assuming δ-function spin waves (blue, dashed) and damped spin waves with damping $\Gamma = 0.03$ meV (red, solid). $|\vec{Q}|$ is the magnitude of the momentum transfer vector parallel to the kagome plane. Error bars and uncertainty values throughout this manuscript are statistical in nature and represent one standard deviation.

We examine the difference in intensities measured at two different applied fields. Since the background and any nonmagnetic scattering signal from the sample should be field-independent, this isolates the signal due to magnetic scattering from the sample. Figure 4(c) shows the model plotted against the data at $|\vec{Q}| = 0.8$ Å^{-1}. The high field data are well fit by this model. At zero field, the spins are aligned parallel to the kagome plane. When the spins are aligned parallel to the kagome plane, the out-of-plane component of the DM vector, D_z, does not contribute to the dispersion. Our measurements taken with the field applied parallel to the kagome plane, shown in Fig. 4(d), are consistent with no contribution from the DM interaction. In both measurements, the peaks are slightly broader than the respective instrumental resolutions, which can be accounted for by including a magnon damping where we replace delta functions in $\mathbf{S}_{\mathrm{SW}}(\vec{\mathbf{Q}}, \omega)$ with Lorentzians and renormalize the magnon frequencies [27]. A Lorentzian half-width at half maximum of $\Gamma = 0.03 \pm 0.01$ meV improves the fit of the calculated $\mathbf{S}_{\mathrm{SW}}(\vec{\mathbf{Q}}, \omega)$ as shown in Fig. 4. Other possible sources of magnon broadening include the imperfect alignment of individual crystals in the measured sample, and further magnetic interactions not included in our model. However, neither of these explain the broadening of the flat mode.

Hence, for the magnon excitations in the kagome-lattice ferromagnet Cu(1,3-bdc), we observe a flat mode that can be gapped from the neighboring dispersive band by the application of a magnetic field perpendicular to the planes. Application of the field parallel to the kagome plane does not open an observable gap. A nearest-neighbor Heisenberg model with DM interaction (which can be mapped to a nearest-neighbor hopping model with spin-orbit interaction) fits the data well. The perpendicular field geometry leads to magnon bands having nonzero Chern number, realizing an example of a topological magnon insulator.

The DM interaction has been shown to drive a magnon Hall effect in a number of ferromagnetic pyrochlore materials [21, 22]. The pyrochlore lattice can be viewed as an alternating stacking of kagome and triangular lattices along the [111] direction. When the magnetic field is applied along the $\hat{z} = [111]$ direction, the projection of the DM vector is zero for bonds between sites of neighboring layers and nonzero and equal for bonds between sites of the same layer. In the limit that interlayer coupling goes to zero, this is precisely the spin Hamiltonian that describes our system.

Therefore, Cu(1,3-bdc) is the first known example of a class of 2D materials that should exhibit two of the most striking phenomena related to spin transport: a magnon Hall ef-

fect [22] and protected chiral edge modes [15]. Thermal conductivity measurements on Cu(1,3-bdc) have been completed [28], and show a bulk magnon Hall effect consistent with the Hamiltonian determined by our neutron scattering measurements [29]. Currently, it is difficult to directly measure the edge modes with inelastic scattering, since current probes either lack the requisite energy resolution (such as resonant x-ray scattering) or intensity from the small edge volume (such as neutron scattering). However, protected chiral edge modes are a consequence of the bulk spin Hamiltonian that describes Cu(1,3-bdc), which is precisely determined by our neutron scattering measurements. Interestingly, in Cu(1,3-bdc), the magnon edge channels can be turned on and off by application of modest magnetic fields. Similar behavior may be found in other kagome ferromagnets, such as the vanadium jarosite $NaV_3(OH)_6(SO_4)_2$ [30]. These materials present a real platform for testing ideas regarding the use of edge magnons to manipulate skyrmions [31], as well as theoretical predictions of hybridization of edge modes [32].

We acknowledge X. G. Wen, P. A. Lee, E. Tang, and J. H. Han for useful discussions. The work at MIT was supported by the US Department of Energy, Office of Science, Office of Basic Energy Sciences under grant no. DE-FG02-07ER46134. D. E. F. acknowledges support from the National Science Foundation, grant no. CHE 1041863. We acknowledge the support of the National Institute of Standards and Technology, U.S. Department of Commerce, in providing the SPINS neutron facility used in this work. Experiments on LET at the ISIS Pulsed Neutron and Muon Source were supported by a beamtime allocation from the Science and Technology Facilities Council.

* robin.chisnell@nist.gov

† youngsl@stanford.edu

[1] K. v. Klitzing, G. Dorda, and M. Pepper, Phys. Rev. Lett. **45**, 494 (1980).

[2] F. D. M. Haldane, Phys. Rev. Lett. **61**, 2015 (1988).

[3] M. Z. Hasan and C. L. Kane, Rev. Mod. Phys. **82**, 3045 (2010).

[4] X.-L. Qi and S.-C. Zhang, Rev. Mod. Phys. **83**, 1057 (2011).

[5] R. Roy and S. L. Sondhi, Physics **4**, 46 (2011).

[6] E. Tang, J. W. Mei, and X. G. Wen, Phys. Rev. Lett. **106**, 236802 (2011).

[7] K. Sun, Z. Gu, H. Katsura, and S. D. Sarma, Phys. Rev. Lett. **106**, 236803 (2011).

[8] T. Neupert, L. Santos, C. Chamon, and C. Mudry, Phys. Rev. Lett. **106**, 236804 (2011).

[9] S. Raghu and F. D. M. Haldane, Phys. Rev. A **78**, 033834 (2008).

[10] Z. Wang, Y. Chong, J. D. Joannopoulos, and M. Soljačić, Nature **461**, 772 (2009).

[11] L. Lu, J. D. Joannopoulos, and M. Soljačić, Nature Photonics **8**, 821 (2014).

[12] N. Y. Yao, A. V. Gorshkov, C. R. Laumann, A. M. Läuchli, J. Ye, and M. D. Lukin, Phys. Rev. Lett **110**, 185302 (2013).

[13] A. Petrescu, A. A. Houck, and K. L. Hur, Phys. Rev. A **86**, 053804 (2012).

[14] J. Koch, A. A. Houck, K. L. Hur, and S. M. Girvin, Phys. Rev. A **82**, 043811 (2010).

[15] L. Zhang, J. Ren, J. S. Wang, and B. Li, Phys. Rev. B **87**, 144101 (2013).

[16] S. Maekawa, *Concepts in Spin Electronics* (Oxford Science Publication, Oxford, 2006).

[17] D. L. Bergman, C. Wu, and L. Balents, Phys. Rev. B **78**, 125104 (2008).

[18] K. Matan, D. Grohol, D. G. Nocera, T. Yildirim, A. B. Harris, S. H. Lee, S. E. Nagler, and Y. S. Lee, Phys. Rev. Lett. **96**, 247201 (2006).

[19] E. A. Nytko, J. S. Helton, P. Müller, and D. G. Nocera, J. Am. Chem. Soc. **130**, 2922 (2008).

[20] H. Katsura, N. Nagaosa, and P. A. Lee, Phys. Rev. Lett. **104**, 066403 (2010).

[21] Y. Onose, T. Ideue, H. Katsura, Y. Shiomi, N. Nagaosa, and Y. Tokura, Science **329**, 297 (2010).

[22] T. Ideue, Y. Onose, H. Katsura, Y. Shiomi, S. Ishiwata, N. Nagaosa, and Y. Tokura, Phys. Rev. B **85**, 134411 (2012).

[23] See Supplemental Materials at [*URL will be inserted by publisher*] for details of sample preparation, measurement configurations, calculations, and Refs.[33-36].

[24] R. I. Bewley, J. W. Taylor, and S. M. Bennington, Nucl. Instrum. Methods **637**, 128 (2011).

[25] T. Moriya, Phys. Rev. **120**, 91 (1960).

[26] T. Holstein and H. Primakoff, Phys. Rev. **58**, 1098 (1940).

[27] G. Shirane, S. M. Shapiro, and J. M. Tranquada, *Neutron Scattering with a Triple-Axis Spectrometer: Basic Techniques* (Cambridge University Press, Cambridge, 2002).

[28] M. Hirschberger, R. Chisnell, Y. S. Lee, and N. P. Ong, Phys. Rev. Lett. **115**, 106603 (2015).

[29] H. Lee, J. H. Han, and P. A. Lee, Phys. Rev. B **91**, 125413 (2015).

[30] D. Grohol, Q. Huang, B. H. Toby, J. W. Lynn, Y. S. Lee, and D. G. Nocera, Phys. Rev. B **68**, 094404 (2003).

[31] M. Pereiro, D. Yudin, J. Chico, C. Etz, O. Eriksson, and A. Bergman, Nat. Comm. **5**, 4815 (2014).

[32] A. Mook, J. Henk, and I. Mertig, Phys. Rev. B **90**, 024412 (2014).

[33] C. K. Loong, S. Ikeda, and J. M. Carpenter, Nucl. Instrum. Methods **260**, 381 (1987).

[34] G. Grosso and G. P. Parravicini, *Solid State Physics* (Academic Press, San Diego, 2003).

[35] S. W. Lovesey, *Theory of Neutron Scattering from Condensed Matter Volume 2: Polarization Effects and Magnetic Scattering* (Clarendon Press, Oxford, 1984).

[36] M. Elhajal, B. Canals, and C. Lacroix, Phys. Rev. B **66**, 014422 (2002).